

# Building Block Syntheses of Gallic Acid Monomers and Tris-(*O*-gallyl)-gallic Acid Dendrimers Chemically Attached to Graphite Powder: A Comparative Study of Their Uptake of Al(III) Ions

Junju Ye,<sup>†</sup> Poobalasingam Abiman,<sup>†</sup> Alison Crossley,<sup>‡</sup> John H. Jones,<sup>§</sup> Gregory G. Wildgoose,<sup>\*,†</sup> and Richard G. Compton<sup>\*,†</sup>

<sup>†</sup>Department of Chemistry, Physical and Theoretical Chemistry Laboratory, University of Oxford, South Parks Road, Oxford, OX1 3QZ United Kingdom, <sup>‡</sup>Materials Department, University of Oxford, Parks Road, Oxford, OX1 3PH United Kingdom, and <sup>§</sup>Chemical Research Laboratory, University of Oxford, Parks Road, Oxford, OX1 3TA United Kingdom

Received July 10, 2009. Revised Manuscript Received September 2, 2009

A synthesis of graphite powder covalently modified with gallic acid (3,4,5-trihydroxybenzoic acid), via a 1,2-diaminoethane “linker” molecule, to form gallylaminoethylaminocarbonyl graphite (gallic-carbon) is reported. The synthesis was used as a model for a “ground-upwards building-block” approach to a primary dendrimer of gallic acid covalently attached to the surface of graphite powder, tris-(*O*-gallyl)-gallylaminoethylaminocarbonyl graphite (TGGA-carbon). The resulting modified carbon materials were characterized at each stage of the syntheses using X-ray photoelectron spectroscopy (XPS) analysis. The effects of increasing the modifier’s structural complexity from monomeric gallic-carbon to the analogous primary dendrimer TGGA-carbon were explored by comparing each material’s efficacy toward the adsorption of Al(III) ions from water. The uptake of Al(III) ions by gallic-carbon and TGGA-carbon was measured using UV–vis spectroscopy. In comparison to the case of monomeric gallic-carbon, the rate of adsorption of Al(III) ions by the TGGA-carbon was found to be 2.3 times more rapid. Furthermore, the total uptake of Al(III) ions was greater (reducing the concentration of 1000 ppb Al(III) solutions to below the WHO legal limit of 100 ppb in less than 5 min) and irreversible, in contrast to the gallic-carbon where the adsorption was found to be under thermodynamic control and to follow a Freundlich isotherm.

## 1. Introduction

Currently, there is much interest in using chemically modified carbon-based materials for a range of applications including, but not limited to, sensors<sup>1–3</sup> and biosensors,<sup>2–4</sup> catalyst supports,<sup>5</sup> and environmental remediation.<sup>6–8</sup> The surface chemistry of graphitic carbon materials is rich, with many synthetically useful functional groups (e.g., carboxyl, hydroxyl or quinonyl moieties) either naturally present or readily introduci- ble.<sup>9–12</sup> The presence of such groups makes carbon a potentially useful, inexpensive support material for solid-phase syntheses. Recently, we have

begun to explore methods of covalently attaching different organic molecules, such as amino acid derivatives,<sup>13–16</sup> polypeptides,<sup>17</sup> aromatic compounds,<sup>18,19</sup> and amino-terminated polyethers (“Jeffamines”)<sup>20</sup> to graphite microparticles. The resulting materials have enabled us to explore various physicochemical properties such as factors influencing the observed changes in surface p*K*<sub>a</sub> of the modifying molecules,<sup>20–22</sup> and to ascertain kinetic<sup>23</sup> and thermodynamic parameters<sup>24,25</sup> controlling the adsorption of several metal ions of environmental concern such as As(III), Cu(II), Cd(II), and Hg(II) by these chemically

\*Corresponding authors. E-mail: gregory.wildgoose@chem.ox.ac.uk (G.G.W.); richard.compton@chem.ox.ac.uk (R.G.C.). Telephone: +44 (0)1865 275406 (G.G.W.); +44 (0)1865 275413 (R.G.C.). Fax: +44 (0)1865 275410

(1) Wildgoose, G. G.; Banks, C. E.; Leventis, H. C.; Compton, R. G. *Microchim. Acta* **2006**, *152*, 187–214.

(2) Gooding, J. J. *Electroanalysis* **2008**, *20*, 573–582.

(3) Wring, S. A.; Hart, J. P. *Analyst* **1992**, *117*, 1215–1229.

(4) Compton, R. G.; Wildgoose, G. G.; Wong, E. L. S. In *Biosensing Using Nanomaterials*; Merkoçi, A., Ed.; Wiley: Hoboken, NJ, 2009.

(5) Wildgoose, G. G.; Banks, C. E.; Compton, R. G. *Small* **2006**, *2*, 182–193.

(6) Jiang, L.; Liu, L.; Luo, X.; Niu, J.; Lu, G. *Huagong Shikan* **2007**, *21*, 64–67.

(7) Moore, E.; Sanvicens, N.; Pravda, M.; Guilbault, G. G. *Int. J. Environ. Anal. Chem.* **2003**, *83*, 545–553.

(8) Yang, B.-Y.; Mo, J.-Y.; Lai, R. *Gaodeng Xuexiao Huaxue Xuebao* **2005**, *26*, 227–230.

(9) Wildgoose, G. G.; Abiman, P.; Compton, R. G. *J. Mater. Chem.* **2009**, *19*, 4875–4886.

(10) Masheter, A. T.; Xiao, L.; Wildgoose, G. G.; Crossley, A.; Jones, J. H.; Compton, R. G. *J. Mater. Chem.* **2007**, *17*, 3515–3524.

(11) Thorogood, C. A.; Wildgoose, G. G.; Crossley, A.; Jacobs, R. M. J.; Jones, J. H.; Compton, R. G. *Chem. Mater.* **2007**, *19*, 4964–4974.

(12) Thorogood, C. A.; Wildgoose, G. G.; Jones, J. H.; Compton, R. G. *New J. Chem.* **2007**, *31*, 958–965.

(13) Wildgoose, G. G.; Leventis, H. C.; Simm, A. O.; Jones, J. H.; Compton, R. G. *Chem. Commun.* **2005**, 3694–3696.

(14) Sljukic, B.; Wildgoose, G. G.; Crossley, A.; Jones, J. H.; Jiang, L.; Jones, T. G. J.; Compton, R. G. *J. Mater. Chem.* **2006**, *16*, 970–976.

(15) Abiman, P.; Wildgoose, G. G.; Crossley, A.; Compton, R. G. *J. Mater. Chem.* **2008**, *18*, 3948–3953.

(16) Abiman, P.; Wildgoose, G. G.; Crossley, A.; Compton, R. G. *Electroanalysis* **2009**, *21*, 897–903.

(17) Wildgoose, G. G.; Leventis, H. C.; Davies, I. J.; Crossley, A.; Lawrence, N. S.; Jiang, L.; Jones, T. G. J.; Compton, R. G. *J. Mater. Chem.* **2005**, *15*, 2375–2382.

(18) Leventis, H. C.; Streeter, I.; Wildgoose, G. G.; Lawrence, N. S.; Jiang, L.; Jones, T. G. J.; Compton, R. G. *Talanta* **2004**, *63*, 1039–1051.

(19) Abiman, P.; Wildgoose, G. G.; Compton, R. G. *J. Phys. Org. Chem.* **2008**, *21*, 433–439.

(20) Abiman, P.; Wildgoose, G. G.; Crossley, A.; Jones, J. H.; Compton, R. G. *Chem.—Eur. J.* **2007**, *13*, 9663–9667.

(21) Abiman, P.; Crossley, A.; Wildgoose, G. G.; Jones, J. H.; Compton, R. G. *Langmuir* **2009**, *25*, 7768.

(22) Masheter, A. T.; Abiman, P.; Wildgoose, G. G.; Wong, E.; Xiao, L.; Rees, N. V.; Taylor, R.; Attard, G. A.; Baron, R.; Crossley, A.; Jones, J. H.; Compton, R. G. *J. Mater. Chem.* **2007**, *17*, 2616–2626.

(23) Chevallier, F. O. G.; Sljukic, B.; Wildgoose, G. G.; Jiang, L.; Jones, T. G. J.; Compton, R. G. *ChemPhysChem* **2006**, *7*, 697–703.

(24) Sljukic, B.; Wildgoose, G. G.; Crossley, A.; Jones, J. H.; Li, J.; Jones, T. G. J.; Compton, R. G. *J. Mater. Chem.* **2006**, *16*, 970–976.

(25) Xiao, L.; Wildgoose, G. G.; Crossley, A.; Knight, R.; Jones, J. H.; Compton, R. G. *Chem.—Asian J.* **2006**, *1*, 614–622.

modified carbon materials from aqueous laboratory solutions and from “real” river and borehole water samples.

The focus of this report is twofold. First, we seek to further develop a “building block” synthetic strategy whereby carbon surfaces are covalently modified with “linker” molecules from which the adsorbent molecules can be attached and built in a “ground upwards” approach to form ever more complex chemical architectures. In doing this, we seek to demonstrate the potential utility of using graphite materials as a support in complex solid-phase synthesis. Second, we seek to examine what are the effects of moving from a monomeric adsorbent attached to an inert graphite carrier to the more complex analogous polymeric or, in this case, primary dendritic structure. How are the thermodynamics and kinetics of adsorption affected? Can we predict the adsorption behavior on moving from a monomeric adsorbent to a dendritic one as has been suggested for certain specific cases by, for example, Crooks and co-workers?<sup>26,27</sup> How do the monomeric and dendritic adsorbent materials compare with one another?

The model modifying compound chosen for this work is gallic acid (3,4,5-hydroxybenzoic acid). Gallic acid is a polyphenolic antioxidant found in many natural products, and like many structurally related polyphenolic compounds, such as pyrocatechol violet (PCV) and tannic acid,<sup>28,29</sup> we demonstrate herein that it is capable of forming complexes with Al(III) ions in aqueous media. Thus, it fulfills our requirements in that the gallic acid molecule can be attached to the carbon surface by coupling the carboxyl group to a 1,2-diaminoethane linker molecule to form gallylaminoethylaminocarbonyl carbon (gallic-carbon). The remaining hydroxyl groups on the gallic acid moiety then allow for further attachment of gallyl moieties to build up a primary dendritic structure (tris-(*O*-gallyl)-gallylaminoethylaminocarbonyl carbon, TGGA-carbon) which is structurally related to tannic acid. The ability of both the gallic-carbon and TGGA-carbon to bind Al(III) ions allows us to then ascertain and compare the factors affecting each material’s adsorption behavior. Note that, although we demonstrate that both materials are capable of rapidly reducing relatively high concentrations of Al(III) ions in water to below the World Health Organization (WHO) legal limits of 100 ppb and 200 ppb set for large and small scale drinking water treatment plants, respectively,<sup>30</sup> we are not claiming to have developed a material for water treatment applications. The laboratory samples used herein are ideal and are unrepresentative of the complex speciation and aquatic chemistry of Al(III) contaminants found in ground and wastewater samples.

## 2. Experimental Section

**2.1. Reagents and Equipment.** All chemicals were of analytical grade and used as obtained from Sigma-Aldrich (U.K.), Fluka (U.K.), or AnalaR (U.K.) without further purification. Synthetic graphite powder, consisting of irregularly shaped particles between 2 and 20  $\mu\text{m}$  in size (measured along the largest axis),<sup>31</sup> was purchased from Aldrich (U.K.). All aqueous solutions were prepared using deionized water from Millipore (Vivendi, U.K.) A UHQ grade water system with a resistivity of

not less than 18.2  $\text{M}\Omega\text{ cm}$  at 25 °C was used. Nonaqueous solvents were dried over 5 Å molecular sieves prior to use. A 100  $\text{mg L}^{-1}$  aluminum(III) stock solution was prepared by dissolving aluminum ammonium disulfate dodecahydrate (< 99.5%, AnalaR) in deionized water. The stock solution was diluted as required.

Voltammetric measurements were performed using a type II  $\mu$ -Autolab (EcoChemie, Utrecht, The Netherlands) computer-controlled potentiostat. All experiments were conducted in a thermostatted (22 °C) three-electrode cell with a solution volume of 20  $\text{cm}^3$  and a three-electrode configuration. The working electrode consisted of a basal-plane pyrolytic graphite electrode (bpgg, Le Carbon, U.K.). The reference electrode was a saturated calomel reference electrode (SCE, Radiometer, Copenhagen, Denmark), and a clean bright platinum coil (99.99% Goodfellow, U.K.) acted as the counter electrode.

X-ray photoelectron spectroscopy (XPS) was performed on a VG Clam 4 MCD analyzer system at the OCMS Begbroke Science Park, University of Oxford, U.K. using X-ray radiation from the Mg K $\alpha$  band ( $h\nu = 1253.6\text{ eV}$ ). All XPS experiments were recorded using an analyzer energy of 100 eV for survey scans and 20 eV for detail scan with a takeoff angle of 90°. The base pressure in the analysis chamber was maintained at not more than  $2.0 \times 10^{-9}$  mbar. Each carbon sample studied was mounted on a stub using double sided adhesive tape and then placed in the ultrahigh vacuum analysis chamber of the spectrometer. Analysis of the resulting spectra was performed using Microcal OriginPro 8. Assignment of spectral peaks was performed using the UKSAF<sup>32</sup> and NIST<sup>33</sup> databases.

pH measurements were made using a pH213 pH meter (Hanna instruments) calibrated using reference buffer solutions of pH  $4.01 \pm 0.01$  and pH  $7.00 \pm 0.01$  (Hamilton).

UV-vis spectroscopy was performed using a model Evolution 60 UV-vis spectrophotometer with VISIONlite Quant version 2.2 software (Thermoscientific). Fourier transform infrared (FT-IR) spectroscopy was performed on a Paragon 1000 (Perkin-Elmer) instrument using KBr plates and nujol as the solvent. <sup>1</sup>H NMR spectroscopy was performed on a Bruker Spectrospin 300 (300 MHz) instrument.

**2.2. Synthetic Methods. 3,4,5-Triacetoxybenzoic Acid.** The synthesis of acetyl-protected gallic acid was adapted from the method of Turner et al.<sup>34</sup> In a 250 mL round-bottom flask, with a magnetic stirrer, were combined gallic acid (5.0 g, 29 mmol) and acetic anhydride (17 mL, 176 mmol, excess). The slurry was stirred as a catalytic amount of sulfuric acid (32  $\mu\text{L}$ ) was added. The temperature rose rapidly from 21 to 75 °C over about 1 min, and the slurry became a clear yellow solution. The mixture was stirred and allowed to cool to room temperature over 20 min. Next 100 mL of water was added to the flask to remove any excess acetic anhydride. After further stirring for 2.5 h, a white crystalline product was isolated by filtration and further washed with 3  $\times$  20 mL aliquots of water. The acetyl-protected gallic acid product was dried in a stream of air for 10 min and then vacuum-dried overnight. From 5.0 g (29 mmol) of gallic acid starting material, we obtained acetyl-protected gallic acid (8.0 g, 93%) as a white crystalline solid, mp 166 °C (lit. 166–168 °C);<sup>34</sup> FT-IR (KBr)  $\nu_{\text{max}}/\text{cm}^{-1}$  1788, 1694, and 1592 (CO);<sup>35</sup>  $\delta_{\text{H}}$  (300 MHz;  $\text{CDCl}_3$ ;  $\text{Me}_4\text{Si}$ ) 2.32 (9 H, s, 3  $\times$  OAc), 7.90 (2H, s, 2  $\times$  ArH);<sup>34</sup> the proton adjacent to the carboxylic group gave a broad peak  $> 12.5$ .<sup>34</sup> Note that the gallic acid starting material does not dissolve in  $\text{CDCl}_3$ .

**Methyl Gallate.** The synthesis of methyl gallate was adapted from the work of Alam et al.<sup>36</sup> and Zhao et al.<sup>37</sup> Gallic acid

(26) Niu, Y.; Sun, L.; Crooks, R. M. *Macromolecules* **2003**, *36*, 5725–5731.

(27) Sun, L.; Crooks, R. M. *J. Phys. Chem. B* **2002**, *106*, 5864–5872.

(28) Haslam, E.; Mills, S. D.; Armitage, R.; Haworth, R. D.; Rogers, H. J.; Searle, T. *J. Chem. Soc.* **1961**, 1836.

(29) Wilson, A. D.; Sergeant, G. A. *Analyst* **1963**, *88*, 109.

(30) *Aluminium in Drinking-water*; W.H.O.: **1998**; [http://www.who.int/water\\_sanitation\\_health/dwq/chemicals/en/aluminium.pdf](http://www.who.int/water_sanitation_health/dwq/chemicals/en/aluminium.pdf).

(31) Wildgoose, G. G.; Wilkins, S. J.; Williams, G. R.; France, R. R.; Carnahan, D. L.; Jiang, L.; Jones, J. H.; Compton, R. G. *ChemPhysChem* **2005**, *6*, 352–362.

(32) <http://www.uksaf.org/>.

(33) <http://srdata.nist.gov/xps/>.

(34) Turner, S. R.; Voit, B. I.; Nielsen, R. B. U.S. Patent 5196502; 1993:496477; CAN 119:96477, **1993**.

(35) Kutani, N. *Chem. Pharm. Bull.* **1960**, *8*, 72–76.

(36) Alam, A.; Takaguchi, Y.; Ito, H.; Yoshida, T.; Tsuboi, S. *Tetrahedron* **2005**, *61*, 1909–1918.

(37) Zhao, Y.; Hao, X. J.; Lu, W.; Cai, J. C.; Yu, H.; Sevenet, T.; Gueritte, F. *J. Nat. Prod.* **2002**, *65*, 902–908.

(5.0 g, 29 mmol) was dissolved in dry methanol (150 mL), to which a catalytic amount (0.3 mL) of concentrated sulfuric acid was carefully added. The solution was heated under reflux for 24 h at 65 °C, after which time the solution was cooled to room temperature and 2.0 M sodium hydroxide was added dropwise until the excess acid had been neutralized. The solvent was removed using a rotary evaporator to yield crude methyl gallate as a white crystalline solid. In order to separate the methyl gallate from any unreacted gallic acid impurities, the product was dissolved in a mixture of ethyl acetate (60 mL) and pure water (20 mL). The organic layer containing the methyl gallate was separated, further washed with pure water (2 × 20 mL) and brine (40 mL), and then dried over magnesium sulfate. The solvent was removed under vacuum, and the product was recrystallized from hot water, before being dried on a high vacuum line to give methyl gallate (2.9 g, 53.5%) as a white crystalline solid, mp 185–188 °C (lit. 188–191 °C<sup>38</sup>); FT-IR (KBr)  $\nu_{\max}/\text{cm}^{-1}$  3340br (OH) 1700, 1618, and 1533(CO);<sup>39</sup>  $\delta_{\text{H}}$  (300 MHz; DMSO-*d*<sub>6</sub>; Me<sub>4</sub>Si) 9.28 (3 H, br s, 3 × OH), 6.91 (2 H, s, 2 × ArH), 3.75 (3 H, s, CO<sub>2</sub>CH<sub>3</sub>).<sup>36,37</sup>

**Methyl Tris-*O*-(tri-*O*-acetylallyl)-gallate.** The method described herein is adapted from the work of Haslam et al.<sup>28</sup> and Nomura et al.<sup>40</sup> 3,4,5-Triacetoxybenzoic acid (2.5 g, 8.43 mmol) was dissolved in chloroform (40 mL), to which excess thionyl chloride (10 mL, 140 mmol) was added. The solution was then heated under reflux at 62 °C for 90 min, after which the chloroform solvent was removed on a rotary evaporator. Any residual thionyl chloride was removed by washing the crude product with dry toluene (2 × 20 mL). The residue thionyl chloride was removed with toluene on a rotary evaporator to give 3,4,5-triacetoxybenzoic chloride as a white crystalline product (2.65 g, 100%). Next, excess 3,4,5-triacetoxybenzyl chloride (3.15 g, 10 mmol) was dissolved in dry dioxane (60 mL) under a nitrogen atmosphere together with methyl gallate (0.46 g, 2.5 mmol) and pyridine (3 mL, 0.037 mmol). The reaction solution was stirred for 4 days, after which time the solvent was removed using a rotary evaporator, and any residual pyridine was removed by washing with dry toluene. The crude product was dissolved in chloroform (60 mL) and washed with 2.0 M NaHSO<sub>4</sub> (20 mL) followed by pure water (2 × 10 mL) and finally brine (40 mL). The organic layer was separated from the aqueous layer and dried over anhydrous sodium sulfate. The solvent was removed under reduced pressure to give methyl tris-*O*-(tri-*O*-acetylallyl)-gallate (2.83 g, 85%) as a pale orange crystalline solid,<sup>28,40</sup> mp 55–58 °C (from chloroform); FT-IR (KBr)  $\nu_{\max}/\text{cm}^{-1}$  1772 (CO);  $\delta_{\text{H}}$  (300 MHz; CDCl<sub>3</sub>; Me<sub>4</sub>Si) 7.78–8.04 (8 H, m, 8 × ArH), 3.73 (3 H, s, OCH<sub>3</sub>), 2.26–2.35 (27 H, m, 9 × OAc).

**Methyl Tris-*O*-gallyl)-gallate.** This procedure was modified from the work of Nomura et al.<sup>40</sup> and Ramesh et al.<sup>41</sup> Methyl tris-*O*-(tri-*O*-acetylallyl)-gallate (2.0 g, 2 mmol) was added to aqueous methanol (1:4 v/v water/methanol, 20 mL) containing ammonium acetate (618 mg, 8.0 mmol). After 6 h, the methyl tris-*O*-(tri-*O*-acetylallyl)-gallate completely dissolved, and the solution was stirred for a further 21 h. After removal of the solvent, the crude product was extracted using aliquots of ethyl acetate (3 × 20 mL). The combined extracts were then dried over anhydrous sodium sulfate, and the solvent removed under reduced pressure to yield pale yellow crystals together with an orange oil. FT-IR and NMR characterization revealed that this product contained the desired product, methyl tris-*O*-gallyl)-gallate (Me-TGG), together with some residual impurities in the orange oil.<sup>40,41</sup> FT-IR (KBr)  $\nu_{\max}/\text{cm}^{-1}$  3400br (OH), 1698 (CO); <sup>1</sup>H

NMR (DMSO-*d*<sub>6</sub>)  $\delta_{\text{H}}$  (300 MHz; DMSO-*d*<sub>6</sub>; Me<sub>4</sub>Si) 9.18 (9 H, br s, 9 × OH), 7.80 (2 H, s, 2 × ArH), 6.63–7.27 (6 H, m, 6 × ArH), 3.73 (3 H, s, CO<sub>2</sub>CH<sub>3</sub>).<sup>40,41</sup>

**1,2-Diaminoethane-Modified Graphite Powder.** Graphite powder (1.2 g, 0.1 mol) was stirred in concentrated nitric acid (21 mL, 0.315 mol) and sulfuric acid (7 mL, 0.126 mol), that is, a 3:1 ratio, for 12 h, washed with a sufficient quantity of pure water until the washings ran neutral, and dried under vacuum. The surface carboxyl groups, **1**, were then converted to more reactive carboxylic acid chloride intermediates, **2**, by stirring the oxidized graphite powder (1.0 g) in thionyl chloride (15 mL, 0.206 mol) at room temperature for 90 min under a nitrogen atmosphere. The excess thionyl chloride was removed under reduced pressure in a rotary evaporator. Next 1,2-diaminoethane (1 mL, 15 mmol) and ethyl diisopropylamine (1.5 mL, 9 mmol) were added to a beaker containing dry dioxane (25 mL), and the solution was then added to the carboxylic acid chloride modified carbon powder in the rotary evaporator (note that the reaction was performed at room temperature to avoid the evaporation of dioxane). After 15 min, the reaction mixture was transferred into a round-bottomed flask with gentle stirring for 18 h under an argon atmosphere to form the 1,2-diaminoethane-modified carbon **3**. This was then washed with dry dioxane and deionized water and dried under vacuum.

**Gallic-Carbon (Gallylaminoethylaminocarbonyl Carbon).** The acetyl-protected gallic acid (3,4,5-triacetoxybenzoic acid, 0.5 g, 1.69 mmol) was converted to the reactive acid chloride derivative using thionyl chloride (15 mL, 0.21 mol) with gentle stirring at room temperature for 90 min under a nitrogen atmosphere. The excess thionyl chloride was again removed under reduced pressure in a rotary evaporator to yield 3,4,5-triacetoxybenzoyl chloride as a pale yellow crystalline solid. Next the 3,4,5-triacetoxybenzoyl chloride, obtained above, was dissolved in dry dioxane (25 mL) in a round-bottomed flask, and then ethyl diisopropylamine (1.5 mL, 9 mmol) and 1.0 g of the 1, 2-diaminoethane-modified carbon powder was added. The reaction mixture was stirred under argon for 18 h, before being filtered, and the solid powder was then washed with dry dioxane followed by deionized water and finally dried under vacuum to yield acetyl-protected gallic-carbon, **6**, as the product.

Finally the acetyl-protecting groups were removed by treating **6** with 0.25 M NaOH solution (25 mL) for 1 h at 58 °C. The product was filtered under suction and washed with copious quantities of water and then acetonitrile, before being dried under vacuum to yield the product, gallylaminoethylaminocarbonyl carbon (gallic-carbon) **7**.

**Tris-*O*-(tri-*O*-acetylallyl)-gallylaminoethylaminocarbonyl Carbon.** A total of 2.5 g (8.43 mmol) of **5** was activated by converting the carboxylic acid group to the corresponding acid chloride as described above. The yellow crystalline product of 3,4,5-triacetoxybenzoyl chloride was dissolved in dry dichloromethane (20 mL). Gallic-carbon (10 g) was suspended in dry dichloromethane (40 mL) containing ethyldiisopropylamine (1.5 mL) under an inert nitrogen atmosphere for 10 min, after which the solution of 3,4,5-triacetoxybenzoyl chloride was slowly added. The reaction suspension was stirred at room temperature for 4 days, after which the modified carbon powder was filtered off and washed with copious quantities of dry dichloromethane, water and acetonitrile, before being dried under vacuum overnight.

**Tris-*O*-gallyl)-gallylaminoethylaminocarbonyl Modified Carbon (TGG A-carbon).** A total of 6 g of the resulting tris-*O*-(tri-*O*-acetylallyl)-gallylaminoethylaminocarbonyl carbon was treated with ammonium acetate to remove the *O*-acetyl protecting groups as described for the solution-phase synthesis of Me-TGG above. The powder was then filtered off, washed with copious quantities of acetonitrile, chloroform, and pure water so as to remove any unreacted species from the carbon surface, and

(38) Kurkin, V. A.; Zapesochnaya, G. G.; Krivenchuk, P. E.; Yurenik, A. Y.; Artamonova, L. P. *Chem. Nat. Prod.* **1984**, *20*, 367–368.

(39) Kuroyanagi, M.; Yamamoto, Y.; Fukushima, S.; Ueno, A.; Noro, T.; Miyase, T. *Chem. Pharm. Bull.* **1982**, *30*, 1602–1608.

(40) Nomura, E.; Hosoda, A.; Morishita, H.; Murakami, A.; Koshimizu, K.; Ohigashi, H.; Taniguchi, H. *Bioorg. Med. Chem.* **2002**, *10*, 1069–1075.

(41) Ramesh, C.; Mahender, G.; Ravindranath, N.; Das, B. *Tetrahedron* **2003**, *59*, 1049–1054.

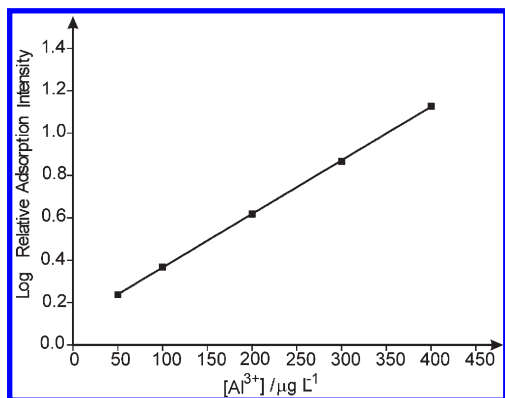


**Figure 1.** Calibration plot made using standard additions of Al(III) of the log of the adsorption intensity (relative to pure water) recorded using UV–vis spectroscopy at a wavelength of 580 nm.

dried to yield the tris-(*O*-gallyl)-gallylaminoethylaminocarbonyl-modified carbon (TGGA-carbon).

**2.3. UV–Vis Spectroscopic Analytical Protocols for Measuring the Concentration of Al(III) Ions.** The concentration of aluminum(III) ions was determined using UV–vis spectrometry by adding excess pyrocatechol violet (PCV) as a colorimetric complexing agent in pH 6.1 buffer, according to literature methods.<sup>29,42,43</sup> The pH 6.1 buffer solution used for UV–vis experiment was prepared by adjusting the pH of a 1.0 M ammonium acetate solution with acetic acid. A stock solution of 0.15% w/w pyrocatechol violet (PCV) indicator for the UV–vis spectroscopic experiments was prepared by dissolving 0.015 g of PCV in 100 mL of deionized water.

A total of 500 μL of PCV and 2.5 mL of buffer solution were added to a 25 mL volumetric flask. Aliquots of either standard additions of known Al(III) concentrations or the sample solutions containing an unknown concentration of Al(III) ions were added, and the solution diluted to 25 mL using pure water, shaken, and allowed to stand for 2 h at 25 °C. Note that the sample solutions were diluted by a factor of 2–25 times depending on the initial Al(III) concentration used so that the concentration of Al(III) ions fell within the linear detection range.<sup>29</sup>

The maximum absorption intensity in the UV–vis spectrum was observed at 580 nm for the Al<sup>3+</sup>–PCV complex and at 450 nm for the free PCV. The adsorption intensity of the Al(III)–PCV complex at 580 nm was measured relative to deionized water in a 1 cm<sup>3</sup> plastic cuvette and was found to obey the Beer–Lambert Law. The Al(III) ion concentration was then determined by comparison to a calibration plot made using known standard concentrations of Al(III) (Figure 1). The intensity of adsorption was found to be proportional to the Al(III) concentration over the range 0–400 ppb, with a limit of detection (determined from 3σ) of <1 ppb. The values of Al(III) ion concentration reported herein that were determined using this method are given as the mean of three repeated measurements in all cases.

### 3. Results and Discussion

The following sections describe the building block syntheses and subsequent characterization of gallic-carbon and TGGA-carbon before each material's behavior toward the adsorption of Al(III) ions is compared.

**3.1. Chemical Modification of Graphite Powder Surface with Gallic Acid.** The first step in the building block synthesis of gallic-carbon (shown in Scheme 1) is to functionalize the graphite support with linker molecules of 1,2-diaminoethane, as described

in section 2.2. In order to improve the coverage of the linker groups on the graphite microparticles, carboxyl groups were first introduced onto the graphite surface via the standard method of acid oxidation.<sup>9,44</sup> This pretreatment is known to increase the surface coverage of carboxyl groups on the graphite powder by as much as between 6 and 10 times that naturally present, corresponding to between ca.  $1 \times 10^{-11}$  and  $2 \times 10^{-11}$  mol cm<sup>-2</sup>.<sup>9,10</sup>

Before coupling the gallic acid groups to the 1,2-diaminoethane-modified carbon, it is first necessary to protect the hydroxyl groups in the gallic acid molecule to prevent unwanted polymerization and side reactions. To this end gallic acid, **4**, was converted to 3,4,5-triacetoxybenzoic acid, **5**, as described in section 2.2. The acetyl-protected gallic acid (0.5 g, 1.69 mmol) was converted to the reactive acid chloride derivative using thionyl chloride and coupled to the 1,2-diaminoethane-modified carbon powder before the acetyl protecting groups were removed to yield gallylaminoethylaminocarbonyl carbon (gallic-carbon, **7**), as detailed in section 2.2 and Scheme 1.

**3.2. Characterization of Gallic-Carbon Powder Using X-ray Photoelectron Spectroscopy.** In order to confirm that each stage of the synthesis of gallic-carbon was successful, X-ray photoelectron spectroscopy (XPS) was carried out on the graphite powder prior to any modification, the oxidized graphite **1**, the 1,2-diaminoethane-modified carbon **3**, acetyl-protected gallic acid modified carbon **6**, and finally the gallic-carbon product **7**. In each case, a wide survey scan was first performed over the range 0–1200 eV for each sample. Next one detailed scan was performed over the C<sub>1s</sub> region, 10 scans over the N<sub>1s</sub> region, and finally 10 scans over the O<sub>1s</sub> region. In some cases, small peaks could be observed corresponding to the trace presence of Ca and Si impurities, most likely arising from the borosilicate glassware during the synthesis. The atomic percentages of C, O, and N elements at each stage of the synthetic procedure are listed in the Table 1.

Figure 2a shows the XPS spectrum of unmodified graphite powder. The two large peaks could be clearly observed at 285 and 533 eV corresponding to the C<sub>1s</sub> and O<sub>1s</sub> emissions, respectively. Repeat scans over the O<sub>1s</sub> region (not shown) revealed a broad peak (530–536 eV) which could not be quantitatively deconvoluted but which qualitatively includes contributions from hydroxyl, quinonyl, and carboxyl surface groups on the carbon surface.<sup>9</sup> A quantitative analysis revealed that the atomic percentage of oxygen on the oxidized graphite surface (Figure 2b) increased to 5.6%, compared to 3.2% in the unmodified graphite (Figure 2a). After modification with 1,2-diaminoethane, a new peak corresponding to emission from the N<sub>1s</sub> level could be observed which was not present in either the blank or oxidized graphite samples. The atomic percentage of nitrogen on the surface was found to be 3.7%.

After coupling the tri-*O*-acetyl-protected gallic acid **6** onto the carbon surface (Figure 2c), a corresponding decrease of the relative atomic percentage of nitrogen was observed, with a corresponding increase in the relative atomic percentage of oxygen atoms, consistent with the stoichiometry of the tri-*O*-acetyl-protected gallic acid molecule. After deprotecting the acetyl groups, one would expect a corresponding decrease in the percentage of oxygen on the surface. Note that Table 1 only reports the absolute atomic percentage of each element, but it is apparent that the percentage of oxygen relative to nitrogen has indeed decreased, which is again consistent with the stoichiometry expected from the final product, gallic-carbon.

(42) Anton, A. *Anal. Chem.* **1960**, *32*, 725–726.

(43) Zhu, X. S.; Bao, L.; Guo, R.; Wu, J. *Anal. Chim. Acta* **2004**, *523*, 43–48.

(44) Marcolino, L. H.; Janegitz, B. C.; Lourenco, B. C.; Fatibello, O. *Anal. Lett.* **2007**, *40*, 3119–3128.

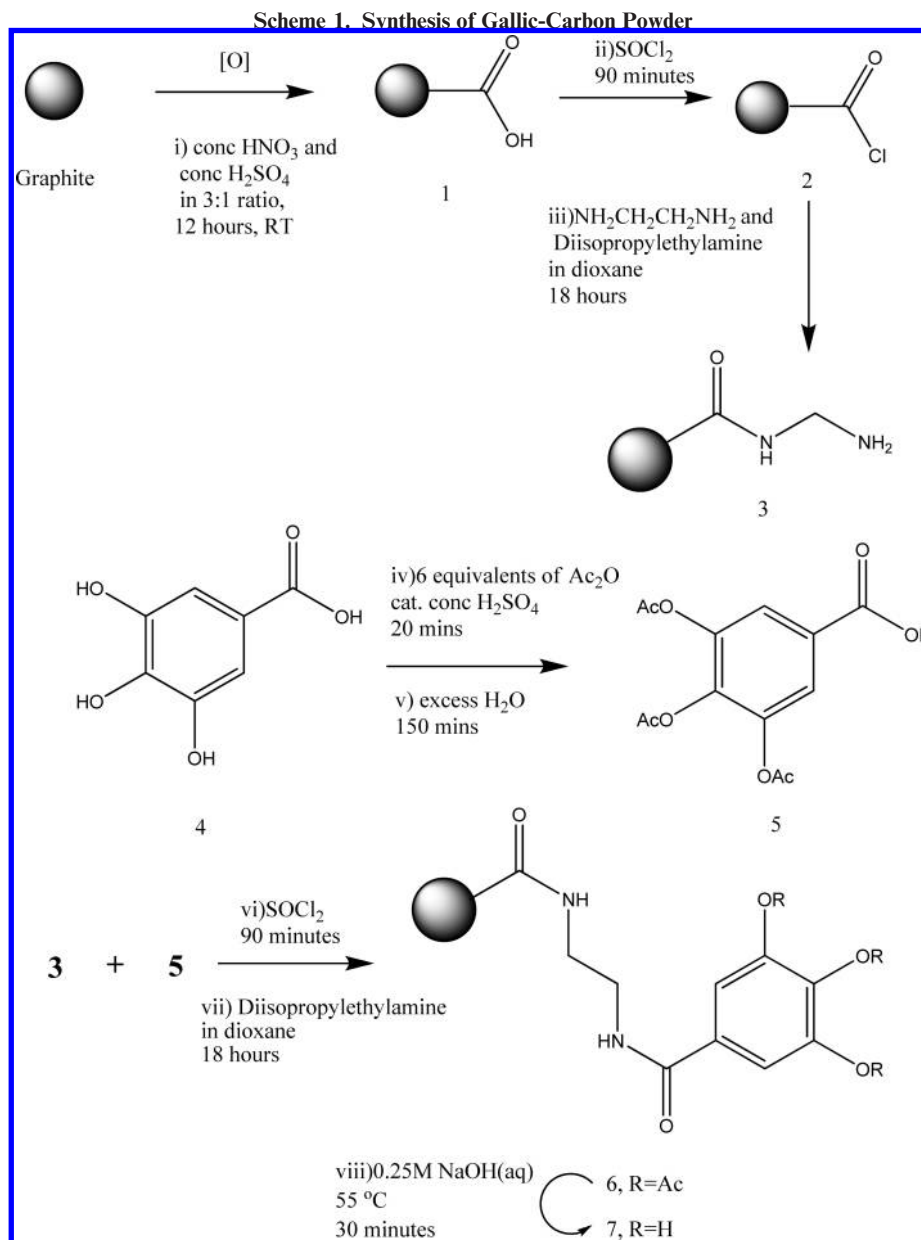


**Table 1. Atomic Percentage Elemental Composition on the Surface of Graphite Powders at Each Stage of the Synthesis of Gallic-Carbon, Determined Using XPS**

sample	% element surface composition		
	N	O	C
unmodified graphite	0.0	3.2	96.9
oxidized graphite	0.0	5.6	94.4
1,2-diaminoethane-modified graphite	3.7	5.1	91.2
tri- <i>O</i> -acetyl gallic modified graphite	1.0	7.2	91.9
gallic-carbon	1.8	7.9	90.3

**3.3. Characterization of Gallic-Carbon Powder Using Cyclic Voltammetry.** In addition to performing XPS characterization, we also carried out characterization of the gallic-carbon, abrasively immobilized onto a bppg working electrode, by comparing its voltammetric response to that of 5 mM gallic acid in pH 4.5 acetate buffer solution (Figure 3). In the case of gallic acid in solution (Figure 3b), the main voltammetric feature of interest is a large, electrochemically irreversible oxidation wave observed at

0.37 V versus SCE, in agreement with the literature.<sup>45</sup> In the case of the gallic-carbon, a reassuringly similar, irreversible oxidation wave is observed upon the first scan at 0.32 V, suggesting that we have successfully modified the carbon surface with gallic acid groups as proposed. Note that the voltammetry of **6** either in solution or attached to the carbon surface did not give rise to any voltammetric signal. The appearance of the irreversible oxidation wave at 0.32 V in the case of gallic-carbon after removal of the acetyl protecting groups provides further evidence to suggest that the deprotection step was successful and resulted in the formation of gallic-carbon.

**3.4. Chemical Modification of Graphite Powder with Tris-(*O*-gallyl)-gallylaminoethylaminocarbonyl Using a “Building Block” Strategy.** In order to synthesize the primary dendrimer of gallic acid, as derivatives of tris-(*O*-gallyl)-gallic acid (TGGA), it is again necessary to use *O*-acetyl protecting groups on the phenolic groups of the incoming gallyl substrate, and to protect the carboxylic acid group of the starting gallic acid

(45) Kilmartin, P. A.; Zou, H. L.; Waterhouse, A. L. *J. Agric. Food Chem.* **2001**, *49*, 1957–1965.

molecule. This is necessary in order to prevent any unwanted or uncontrolled self-condensation reactions and polymerization to form dendrimers closely related to tannic acid derivatives. The

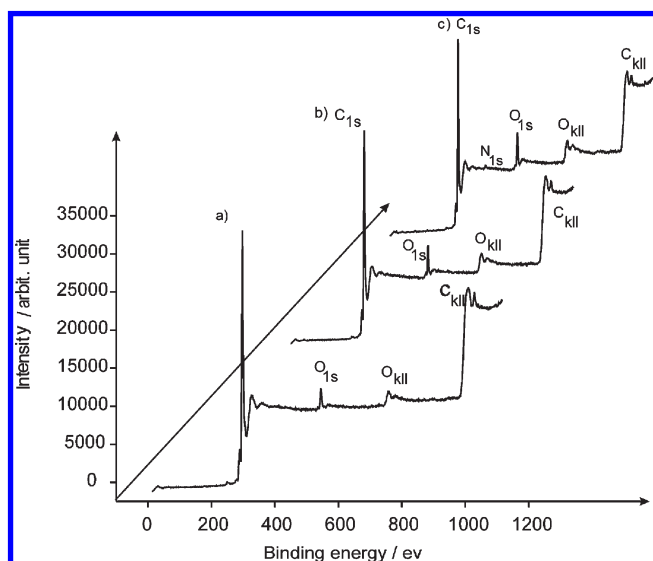


**Figure 2.** XPS spectra (wide scans 0–1200 eV) of (a) unmodified graphite powder, (b) oxidized graphite powder, and (c) tri-*O*-acetyl gallic-carbon powder.

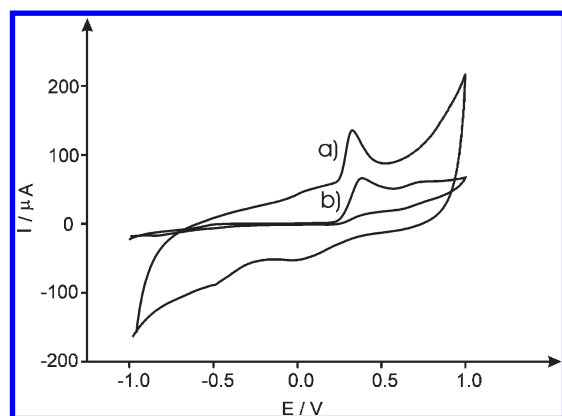


**Figure 3.** First scan cyclic voltammograms (scanning from  $-1$  V to  $+1$  V versus SCE; scan rate,  $100 \text{ mV s}^{-1}$ ) recorded in pH 4.5 acetate buffer solution of (a) gallic-carbon powder abrasively immobilized on the surface of a bppg electrode and (b) 5 mM gallic acid in pH 4.5 buffer solution.

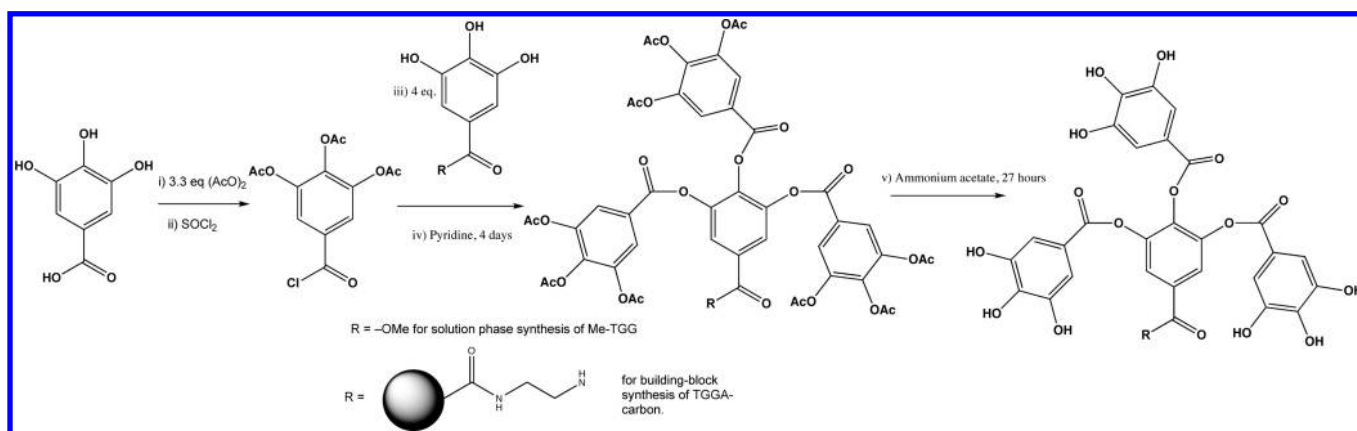
difficulty then lies in selectively removing the *O*-acetyl protecting groups while leaving the gallyl-gallate linkages intact. We therefore decided to check the selectivity of our deprotection method in a solution phase synthesis of methyl tris-(*O*-gallyl)-gallate (Me-TGG), where characterization of the obtained product using standard  $^1\text{H}$  NMR and FT-IR techniques could be performed. The synthesis of Me-TGG is shown in Scheme 2 and detailed in section 2.2. Characterization of the resulting Me-TGG product (section 2.2) confirmed that we had successfully synthesized Me-TGG, and that the mild hydrolysis conditions used were selective for the removal of the *O*-acetyl protecting groups in preference to cleavage of the gallyl-gallate ester linkages.<sup>41</sup>

Having confirmed that our proposed synthetic strategy allows us to obtain primary dendrimers of gallic acid in the form of Me-TGG, we next attempted to chemically modify the surface of graphite powder with TGGa. However, instead of first synthesizing TGGa and then attempting to couple this large, sterically hindered molecule to the 1,2-diaminoethane linker attached to the graphite powder (which is itself severely sterically hindered on the graphite particle surface and present at a relatively low surface concentration), we decided to synthesize the TGGa-carbon powder starting from gallic acid modified carbon powder (gallic-carbon), that we successfully synthesized above, and further extending the “building-block” synthesis as shown in Scheme 2 and detailed in section 2.2. As the gallic acid derivatives used in this synthesis are much more soluble in the chosen solvents than TGGa, any unreacted material is likely more easily removed from the carbon surface than would be the case if we attempted to couple TGGa onto the surface directly. Thus, we can be confident that only chemically attached TGGa dendrimers will be formed on the carbon surface without any physisorbed materials giving rise to possible misinterpretation of our experimental data.

Again, the deprotection of the tri-*O*-acetylgallyl groups, contained in the tris-(*O*-(tri-*O*-acetylgallyl)-gallylaminoethylamino-carbonyl carbon intermediate (Scheme 2), was achieved using the mild hydrolysis conditions successfully developed in the solution phase synthesis of MeTGG described above.

**3.5. Characterization of TGGa-Carbon Using X-ray Photoelectron Spectroscopy.** In order to confirm that each stage of the synthesis of TGGa-carbon had been successful, XPS analysis was performed on the tri-*O*-acetyl-protected gallic-carbon, gallic-carbon, tris-(*O*-(tri-*O*-acetylgallyl)-gallylaminoethylamino-carbonyl carbon, and finally the TGGa-carbon product. A wide survey scan was performed for each sample from 0 to 1200 eV as shown in Figure 4, and detailed scans over the  $\text{C}_{1s}$ ,  $\text{O}_{1s}$ , and  $\text{N}_{1s}$  regions of interest. As expected, C, O, and N were the

**Scheme 2. Synthetic Route to Me-TGG (Solution Phase) or Alternatively TGGa-Carbon (Solid-Phase Building-Block Synthesis)**



only elements observed to be present on the surface with the occasional exception of trace ( $<0.2$  atomic %) Si impurities arising from the borosilicate glassware. Table 2 details the absolute atomic percentage of each element, C, O, and N, on the surface of each sample determined from the area under each peak. The chemical environment of carbon and oxygen atoms within the gallyl moieties of the dendrimer are very similar to those atoms in surface oxo-groups decorating the edges of the graphene sheets,<sup>9–12</sup> and therefore prevents detailed deconvolution and analysis of either the  $C_{1s}$  or  $O_{1s}$  peak. Furthermore, as each stage of the building-block synthesis involves changing the number of both carbon and oxygen atoms to the surface, we cannot follow the synthesis using the absolute surface percentage corresponding to each element. Fortunately, the number of nitrogen atoms on the surface is not affected by the modification

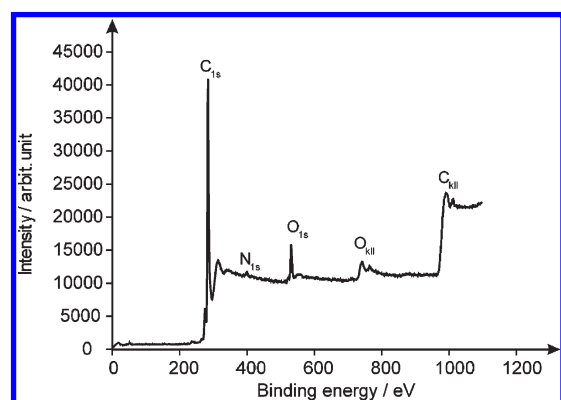


**Figure 4.** Wide survey XPS spectrum of TGGA-carbon.

chemistry. Therefore, the area of the  $N_{1s}$  signal was used as a “marker” and, knowing the modifying molecules’ stoichiometry (and remembering to correct for the relative atomic sensitivity factors<sup>32</sup>), can be used to decouple the percentage of the  $C_{1s}$  and  $O_{1s}$  peak area attributable to the modifying molecules from the background oxygen and carbon signals arising from the graphite support. The resulting values are detailed in Table 2.

Having ascertained the relative atomic surface percentage of each element at every stage of the synthesis, it is instructive to compare the ratios of carbon and oxygen atoms relative to gallic-carbon predicted from the stoichiometry of each moiety as we proceed through the synthesis with the experimentally obtained ratios (Table 3). As an illustrative example of this, the gallic-carbon, to which we refer each ratio to, contains 2 nitrogen atoms, 10 carbon atoms (including the carbonyl carbon to which the 1,2-diamino linker forms an amide bond to the carbon surface and the 2 carbons in the ethyl chain of this linker group), and 5 oxygen atoms. Consider the tri-*O*-acetyl-protected precursor of the gallic-carbon. This now has 16 carbon atoms and 8 oxygen atoms, resulting in a stoichiometric ratio of 1.6 for both of these elements. Also listed in Table 3 are the stoichiometric ratios predicted if we had formed mono- and bis-(*O*-gallyl)-gallylaminoethylaminocarbonyl groups on the graphite surface. In comparison to the possible mono- and bis-(*O*-gallyl)-gallylaminoethylaminocarbonyl structures, and within the limit of experimental error, the XPS data give ratios for both the change in carbon and oxygen atoms relative to gallic-carbon that are not inconsistent with the formation of the desired TGGA-carbon product together with the possible formation of some bis-(*O*-gallyl)-gallylaminoethylaminocarbonyl carbon.

**Table 2. Absolute Elemental Percentage of C, O, and N Atoms on the Surface of Each Modified Carbon Sample Determined Using XPS<sup>a</sup>**

material	absolute elemental percentage			percentage of the absolute signal attributable to atoms in the modifier	
	C%	O%	N%	C%	O%
tri- <i>O</i> -acetyl gallic-carbon	93.5	6.0	0.5	8.0	1.5
gallic-carbon	93.9	5.3	0.7	6.0	1.1
tris- <i>O</i> -(tri- <i>O</i> -acetyl-gallyl)-gallylaminoethylaminocarbonyl-carbon	92.3	7.0	0.6	22.3	4.6
TGGA-carbon	93.0	5.8	1.0	24.6	5.1

<sup>a</sup>Note that trace Si impurities ( $<0.2\%$ ) occasionally observed are not included. Also included is the decoupled percentage of the absolute C and O signal attributable to atoms within the modifying molecules (determined using the  $N_{1s}$  peak as a “marker”, see text).

**Table 3. Comparison of the Predicted and Experimentally Observed Stoichiometric Ratios of C and O Atoms for Each Material Relative to the Number of C and O Atoms in Gallic-Carbon As Determined from XPS<sup>a</sup>**

material	predicted stoichiometric atomic ratio relative to gallic-carbon		experimental stoichiometric atomic ratio determined from XPS	
	C	O	C	O
gallic-carbon	1.0	1.0	1.0	1.0
tri- <i>O</i> -acetyl gallic-carbon	1.6	1.6	1.3	1.4
tris- <i>O</i> -(tri- <i>O</i> -acetyl-gallyl)-gallylaminoethylaminocarbonyl-carbon	4.9	5.2	3.7	4.2
TGGA-carbon	3.1	3.4	4.1	4.6
bis- <i>O</i> -(tri- <i>O</i> -acetyl-gallyl)-gallylaminoethylaminocarbonyl-carbon	3.6	3.8		
bis-( <i>O</i> -gallyl)-gallylaminoethylaminocarbonyl-carbon	2.4	2.6		
mono- <i>O</i> -(tri- <i>O</i> -acetyl-gallyl)-gallylaminoethylaminocarbonyl-carbon	2.3	2.4		
mono-( <i>O</i> -gallyl)-gallylaminoethylaminocarbonyl-carbon	1.7	1.8		

<sup>a</sup>Also included are the predicted stoichiometric ratios for the related bis- and mono-(*O*-gallyl)-gallylaminoethylaminocarbonyl carbon structures.

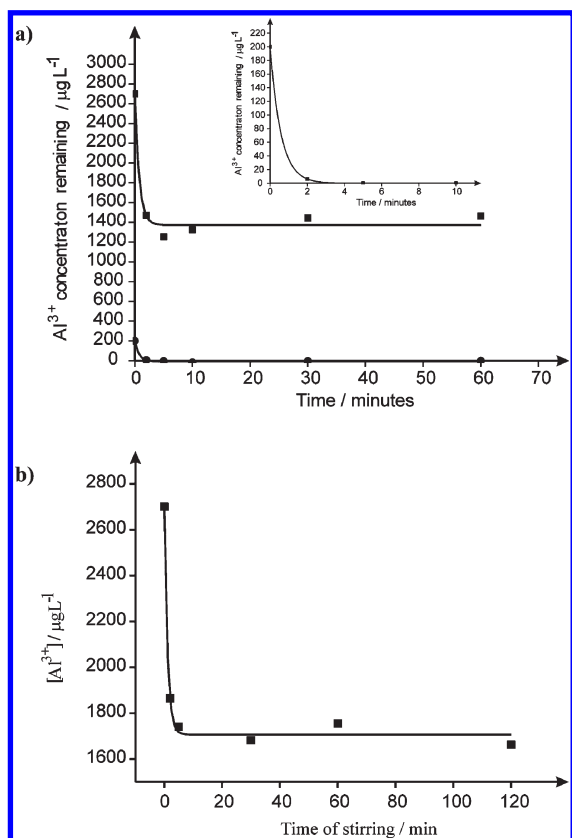


**Figure 5.** Plot of the concentration of Al(III) ions remaining in solution after treatment for varying lengths of time with (a) 200 mg of TGGA-carbon powder with an initial Al(III) concentration of 2700 and 200  $\mu\text{g L}^{-1}$  (inset: enlarged view of the data starting from an initial Al(III) concentration of 200  $\mu\text{g L}^{-1}$ ) and (b) 200 mg of gallic-carbon powder with an initial Al(III) concentration of 2700  $\mu\text{g L}^{-1}$ .

**3.6. A Comparison of the Adsorption of Al(III) Ions by Gallic-Carbon and TGGA-Carbon.** In order to evaluate and compare the efficacy of gallic-carbon and TGGA-carbon toward the removal of Al(III) ions from aqueous media, the concentration of Al(III) ions present in any given sample, before and after exposure to gallic-carbon, was determined using UV-vis spectroscopy, as described in section 2.3. The kinetic and, where appropriate, thermodynamic parameters controlling the adsorption of Al(III) ions by each material studied were ascertained as follows.

**3.6.1. Investigating the Kinetics of Al(III) Adsorption.** In order to ascertain the rate of adsorption of Al(III) ions by either gallic-carbon or TGGA-carbon, 25 mL of either a 2700  $\mu\text{g L}^{-1}$  or a 200  $\mu\text{g L}^{-1}$  Al(III) solution was separately stirred with 200 mg of each modified carbon powder for varying lengths of time. The modified carbon powders were then removed by filtration, and the concentration of Al(III) ions remaining in the solution was determined using UV-vis spectroscopy. Figure 5 reveals that the adsorption of Al(III) ions from the solution occurred rapidly within the first 5 min for both gallic-carbon and TGGA-carbon, after which no further adsorption occurred. In the case where the initial Al(III) concentration was 2700  $\mu\text{g L}^{-1}$ , the concentration was reduced to ca. 1400  $\mu\text{g L}^{-1}$  within the first 5 min of stirring with TGGA carbon, while for the 200  $\mu\text{g L}^{-1}$  solution the concentration of Al(III) ions was reduced to below the detection limit in the same time. Comparing this to the performance of gallic-carbon, where the concentration of Al(III) ions remaining

**Table 4. Quantitative Analysis of the Concentration of Al(III) Ions Remaining in Solution after Exposure to 200 mg of Gallic-Carbon Powder for 30 min**

initial concentration of Al(III)/ $\mu\text{g L}^{-1}$	Al(III) ion concentration remaining in solution/ $\mu\text{g L}^{-1}$
270	51
675	107
945	183
1350	333
2700	1671

**Table 5. Quantitative Analysis of the Concentration of Al(III) Ions Remaining in Solution after 30 min of Stirring with 200 mg of TGGA-Carbon Powder**

Initial concentration of Al(III)/ $\mu\text{g L}^{-1}$	Al(III) ion concentration remaining in solution/ $\mu\text{g L}^{-1}$
200	< L.O.D.
500	6
1000	416
2700	1443

after 5 min of stirring was 1671 and 51  $\mu\text{g L}^{-1}$  for an initial concentration of 2700 and 200  $\mu\text{g L}^{-1}$ , respectively, it is apparent that the TGGA-carbon is more effective at removing Al(III) ions, especially from solutions close to the WHO legal limit of 200 ppb, where effectively all of the Al(III) ions are removed. In a series of control experiments using unmodified graphite powder under identical conditions, no adsorption of Al(III) ions was observed.

Furthermore, if we compare the rate of adsorption by the TGGA-carbon with that of gallic-carbon, using theory developed by Chevallier et al.,<sup>23</sup> the *minimum* rate of adsorption of Al(III) by TGGA-carbon was found to be  $3.86 \times 10^{-4} \text{ cm s}^{-1}$  compared to  $1.72 \times 10^{-4} \text{ cm s}^{-1}$  determined for gallic-carbon. We note that the rate of adsorption in the Chevallier model is first order with respect to the number of surface sites available for complexation and that the minimum rate of adsorption of TGGA-carbon is 2.25 times of that of gallic-carbon. This is therefore consistent with an increased number of gallic acid moieties available in the dendritic TGGA molecule to complex the Al(III) ions, and the ratio of ca. 2.3:1 for TGGA-carbon/gallic-carbon is consistent with the results of XPS characterization in that the TGGA-carbon likely consists of a mixture of tris- and bis-(*O*-gallyl)-gallylaminoethyl-aminocarbonyl groups on the carbon surface.

**3.6.2. Investigating the Adsorption of Al(III) Ions of Different Initial Concentrations with a Constant Mass of Either Gallic-Carbon or TGGA-Carbon.** As stated in the Introduction, we are interested in comparing how the adsorption efficacy and the parameters controlling the uptake of adsorbates vary between monomeric and dendritic forms of adsorbents. Therefore, 25 mL aliquots of Al(III) solutions with concentrations ranging from 200 to 2700  $\mu\text{g L}^{-1}$  Al(III) ions were prepared by diluting the stock solution appropriately. Each sample was separately stirred with 200 mg of either gallic-carbon or TGGA-carbon powder for a period of 30 min, after which the modified carbon powder was removed by filtration and the Al(III) concentration remaining in the filtrate was determined, the results of which are shown in Tables 4 and 5 for gallic-carbon and TGGA-carbon, respectively.

The capacity of the adsorbent and the equilibrium relationships between adsorbate and adsorbent can be described by adsorption isotherms, of which the Langmuir and Freundlich isotherms were the earliest and simplest relationships used. The data obtained in Tables 4 and 5 were therefore analyzed using linearized forms of both the Langmuir isotherm and the Freundlich isotherm. None

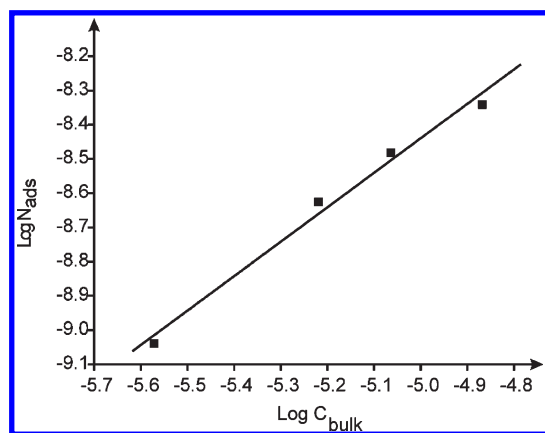


**Figure 6.** Freundlich plot for the uptake of Al(III) ions from solutions of different initial concentration by 200 mg of gallic-carbon powder.

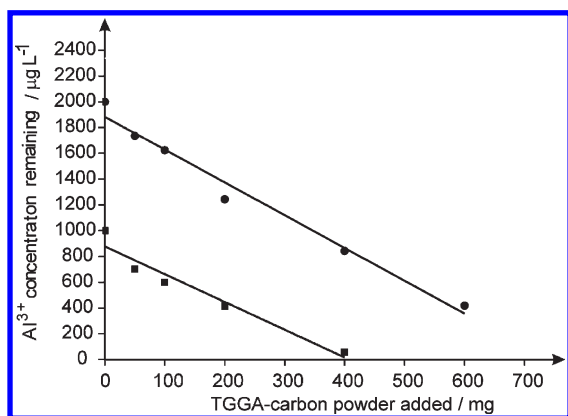


**Figure 7.** Plot of the concentration of Al(III) remaining in the solution after 30 min of stirring with TGGA-carbon powder versus the mass of TGGA-carbon added for two initial concentrations of Al(III) of 1000 and 2000  $\mu\text{g L}^{-1}$ .

of the data obtained for either gallic-carbon or TGGA-carbon were found to conform to the Langmuir isotherm.

In the case of gallic-carbon, the data in Table 4 were found to fit to the linearized form of the Freundlich equation given by eq 1:

$$\log N_{\text{ads}} = \log K + \frac{1}{n} \log C \quad (1)$$

where  $N_{\text{ads}}$  is the metal ions uptake, described by the mass of Al(III) ions adsorbed per milligram of gallic-carbon powder,  $C$  is the concentration of Al(III) remaining in the solution, and  $K$  and  $n$  are Freundlich constants relating to the maximum adsorption capacity and adsorption intensity, respectively. The larger the value of  $K$  and the smaller the value of  $n$  (which typically takes values from 1 to 10), the higher the affinity of the adsorbent toward the adsorbate. Fitting the experimentally determined data to the Freundlich isotherm in the case of gallic-carbon gave a linear relationship ( $R^2 = 0.98$ ), shown in Figure 6. From this plot, the values of  $K$  and  $n$  were determined to be  $K = 0.38 \text{ L g}^{-1}$  and  $n = 0.99$ , which is comparable to our previous studies involving the adsorption of other metal ions such as Cu(II) and Cd(II) using carbon powders chemically modified with monomeric adsorbents.<sup>14,16</sup>

In contrast to the adsorption behavior of gallic-carbon, it is immediately apparent from Table 5 that 200 mg of TGGA-carbon reduces the concentration of Al(III) ions by ca. 500  $\mu\text{g L}^{-1}$  regardless of the initial Al(III) ion concentration.

This is not consistent with the adsorption process following a thermodynamically controlled adsorption isotherm, and it appears that the TGGA-carbon is simply “titrating” the Al(III) ions from solution. Repeat experiments at an elevated temperature of 40 °C gave similar results for the amount of Al(III) ions removed by TGGA-carbon, again suggesting that the adsorption is not under thermodynamic control and is, in effect, an irreversible titration. To confirm this, 25 mL of two Al(III) solutions with an initial concentration of 1000 and 2000  $\mu\text{g L}^{-1}$  were separately exposed to increasing amounts of TGGA-carbon powder (25, 50, 200, 400, and 600 mg). The corresponding plot of concentration of Al(III) remaining in the solution after 30 min of stirring with TGGA-carbon powder versus the mass of TGGA-carbon added is shown in Figure 7. From this, it is clearly apparent that the TGGA-carbon powder is simply “titrating” the Al(III) ions from solution and that the adsorption behavior of the primary dendrimer adsorbent, at least toward Al(III) ions under the conditions used herein, differs markedly and perhaps unexpectedly from that of the monomeric form of the adsorbent material, that is, gallic-carbon. Note that, in the case where the initial concentration of Al(III) was 1000  $\mu\text{g L}^{-1}$ , exposure to 400 mg of TGGA-carbon powder reduced the concentration to 56  $\mu\text{g L}^{-1}$ . This is lower than the upper WHO legal limit (200 ppb) for small-scale water treatment plants and indeed lower than the more stringent legal limit set for drinking water supplies and large-scale water treatment facilities (100 ppb), with the caveat that these are laboratory samples not “real” sample matrices where the speciation of Al(III) ions is more complex as mentioned in the Introduction. Note that the titration data above correspond to the removal of ca. 2.2  $\mu\text{mol}$  of  $\text{Al}^{3+}$  ions per gram of TGGA-carbon and imply a loading of ca. 0.7  $\mu\text{mol}$  of dendron per gram of modified carbon material or approximately  $1 \times 10^{-12} \text{ mol cm}^{-2}$ .

#### 4. Conclusions

Synthetic protocols for the covalent attachment of gallic acid molecules to the surface of graphite microparticles, the solution phase synthesis of TGGA (a primary dendrimer of gallic acid), and the solid-phase synthesis of TGGA covalently attached to graphite microparticles in a ground-upward “building-block” fashion are reported. Characterization of the successful synthesis of TGGA in the solution phase was performed using standard  $^1\text{H}$  NMR and FT-IR characterization techniques. The synthesis of gallic-carbon and TGGA-carbon powders was followed at each stage of the procedure using XPS. In the case of the TGGA-carbon material, XPS characterization suggested that the material consisted of a mixture of both tris- and some bis-(*O*-gallyl)-gallylaminoethylaminocarbonyl moieties on the carbon surface.

The efficacy of the gallic-carbon and TGGA-carbon powders toward the removal of Al(III) ions from aqueous solutions was then examined and compared using UV-vis spectroscopy. Both gallic-carbon and TGGA-carbon were found to exhibit rapid kinetics for the uptake of Al(III) ions, fully occurring within 5 min of exposure of the sample to the modified carbon powders. The kinetics of adsorption were investigated, and the adsorption rate constants were found to be  $3.86 \times 10^{-4}$  and  $1.72 \times 10^{-4} \text{ cm}^{-1}$  for TGGA-carbon and gallic-carbon, respectively. Thus, TGGA-carbon adsorbs Al(III) ions 2.3 times faster, consistent with the increased number of adsorption sites in the dendritic form of gallic acid and confirming the results of XPS characterization in that the TGGA-carbon may actually consist of a mixture of

both tris- and some bis-(*O*-gallyl)-gallylaminoethylaminocarbonyl moieties on the carbon surface.

While the adsorption of Al(III) ions by gallic-carbon was found to be reversible and to obey a Freundlich isotherm, adsorption by the TGGA-carbon was irreversible. The TGGA-carbon simply titrates Al(III) ions from solution, with Al(III) concentrations below the WHO limits obtainable from laboratory solutions with initial concentrations of  $500 \mu\text{gL}^{-1}$  within 5 min of exposure. It would appear that forming dendrimers or polymers of adsorbent materials on solid supports may, in certain cases, such as the comparison made herein between gallic acid and TGGA groups on graphite powder, drastically alter their adsorption behavior.

We believe that graphitic carbon materials show great promise as relatively inexpensive supports for solid-phase

synthesis, and we have demonstrated that relatively complex chemical architectures can be constructed, and selective chemistries can be readily performed on their surface. Issues with relative loading of modifying molecules on these support materials are yet to be overcome, and this is an ongoing area of our research. The TGGA-carbon material shows promise as an inexpensive and easy way to make material. Polyphenolic compounds, such as gallic acid and TGGA, may complex other trivalent metal ions of greater environmental concern than Al(III), and this is an area of ongoing investigation in our laboratory.

**Acknowledgment.** G.G.W. thanks St. John's College for support via a Junior Research Fellowship.